



Original Research

SPARC is a Novel Prognostic Biomarker for Ovarian Cancer and Associated with Immune Signatures and Drug Response

Xiaorong Guo^{1,†}, Huilin Tai^{2,†}, Xiaoqing Li^{1,†}, Peng Liu³, Jin Liu¹, Shan Yu^{1,*}

¹Department of Pathology, Second Affiliated Hospital of Harbin Medical University, 150086 Harbin, Heilongjiang, China

²Department of Mathematics and Statistics, McGill University, Montreal, QC H3A 0G4, Canada

³Laboratory of Medical Genetics, Harbin Medical University, 150086 Harbin, Heilongjiang, China

*Correspondence: yushan@hrbmu.edu.cn (Shan Yu)

†These authors contributed equally.

Academic Editor: Valerio Gaetano Vellone

Submitted: 8 October 2023 Revised: 2 December 2023 Accepted: 12 December 2023 Published: 6 March 2024

Abstract

Background: The calcium-binding matricellular glycoprotein (SPARC, secreted protein, acidic and rich in cysteine) belongs to the extracellular-matrix-protein family, and its functions mainly focus on tissue injury, remodeling, and tumorigenesis. The role of SPARC in ovarian cancer remains controversial at present. **Methods:** We searched SPARC using The Cancer Genome Atlas/Genotype-Tissue Expression (TCGA/GTEX) and other databases to analyze the relationship between its expression level and survival, immunity signatures, and chemical drug response, in ovarian cancer. Additionally, we overexpressed SPARC with plasmids in ovarian cancer SKOV3 and ID8 cell lines, then measured the effects of SPARC on the proliferation, migration, invasiveness, clonality, and stemness of ovarian cancer cells by Cell Counting Kit-8 (CCK8), Transwell, wound healing assay, adhesion assay, plate cloning assay, and soft agar spheroid formation *in vitro*. The Gene Ontology (GO) and Kyoto Encyclopedia of Genes and Genomes (KEGG) enrichment analyses showed the potential signaling pathway for SPARC. **Results:** The higher expression of SPARC in ovarian cancer is related to more advanced tumor stage, poorer clinical survival, and worse chemical drug response, whereas it is positively correlated with immune signatures. For ovarian cancer phenotypes, higher SPARC expression level promotes cell proliferation, migration, colony formation, and spheroid formation. The GO and KEGG enrichment highlighted the potential molecular mechanisms for SPARC with PI3K-AKT and MAPK signaling regulation. **Conclusions:** SPARC promotes ovarian cancer progression through proliferation, migration, invasiveness, clonality, and stemness. A high level of expression of SPARC in ovarian cancer patients can be used as a marker of poor prognosis and poor drug response.

Keywords: drug response; immune cell infiltration; metastasis; ovarian cancer; SPARC

1. Introduction

SPARC (secreted protein, acidic and rich in cysteine), also known as osteonectin or BM-40, is a multifunctional glycoprotein (32–35 kDa) that belongs to the extracellular-matrix-protein family. It is encoded by a single gene on human chromosome 5q31.1 [1,2]. The mature SPARC protein is composed of three different regions, which include an N-terminus acidic domain (NT), a follistatin-like domain (FS), and a C-terminus domain (EC). The NT domain contains a Ca²⁺ binding domain with low affinity. There are several internal disulfide bonds and N-glycosylation sites in the FS domain. The EC domain contains peptide sequences and collagen-binding domains capable of inhibiting endothelial cell proliferation [3]. SPARC has been linked to cancer, tissue remodeling, and damage. It binds with extracellular matrix (ECM) components to control cell adhesion, proliferation, migration, and growth factor signaling, but does not function as an ECM component [1,2].

According to the The Cancer Genome Atlas (TCGA) database, the *SPARC* gene is expressed in 32 different forms of cancer, and patients with breast cancer, gastric adenocarcinoma, pancreatic cancer, and mesothelioma have a poor

prognosis when this gene is highly expressed [3–5]. The overexpression of SPARC has been shown to enhance liver cancer cell (HepG2 cell) proliferation *in vitro* and tumor growth in murine xenograft models [6]. SPARC acts as a mediator of transforming growth factor beta1 (TGF- β 1) signaling, thus inducing epithelial-mesenchymal transition (EMT) in different malignancies such as lung, breast, and renal cancer [6–8]. SPARC also enhances EMT in head and neck cancers by activating the AKT pathway [9].

However, there is some debate about the roles of SPARC in human malignancies. In colorectal, prostate, and cervical cancer, SPARC is considered to act as a tumor suppressor [10]. Research has suggested that SPARC is involved in inducing endoplasmic reticulum (ER) stress to promote autophagy-mediated apoptosis in neuroblastoma [11]. In addition, SPARC has been found to reduce bladder cancer proliferation and lung metastasis by inhibiting cancer-associated inflammation [12].

The roles of SPARC in ovarian carcinomas are unclear. Some reports have suggested that SPARC may have pro-tumor effects in ovarian cancer and some suggested anti-tumor effects. Chen *et al.* [13] showed that decreas-



ing SPARC could inhibit ovarian cancer growth, accelerate apoptosis, and suppress metastasis and invasion. On the other hand, research has shown that SPARC can inhibit peritoneal metastasis of ovarian cancer cells by inhibiting the cEBP β -NF κ B-AP-1 transcription machinery [14]. Yet other evidence supported the idea that SPARC normalizes the ovarian cancer microenvironment via regulating VEGF-integrin-MMP axis [15].

In the present study on ovarian cancer, we sought to validate SPARC expression-based function in cell proliferation, migration, invasiveness, clonality and stemness, *in vitro*.

2. Materials and Methods

2.1 Cell Lines

The SKOV3 and ID8 cell lines were obtained from ATCC and Sigma-Aldrich, respectively. We tested for mycoplasma contamination and verified cells by short tandem repeat (STR) test; morphology was confirmed by pathologist before the experiments. Cells were cultured in DMEM medium mixed with 10% fetal bovine serum (Biosharp, Hefei, Anhui, China), 100 U/mL penicillin, and 100 U/mL streptomycin (Phygene, Fuzhou, Fujian, China) at 37 °C with 5% CO₂.

2.2 Cell Transfection

The SPARC over-expressing plasmid was synthesized and the coding area of SPARC, based on pcDNA3.1+ vector, was added. The SPARC-over-expression (OE) vector was transfected into SKOV3 cells and ID8 cells by Lipofectamine 8000 (Beyotime, Shanghai, China). The empty plasmid was also transfected as the internal control.

2.3 Wound Healing Assay

SKOV3-Vector/ID8-Vector cells and SKOV3-SPARC/ID8-SPARC cells (4×10^5) were grown in 6-well plates to a density greater than 90%. A single scratch in the center of the plate was made by a p1250 pipette tip. After 24 h, photomicrographs were taken through a light microscope (EVOS, ThermoFisher, Waltham, MA, USA). The cell merging front was calculated by ImageJ (version 1.54f, LOCI, University of Wisconsin, Madison, WI, USA).

2.4 Colony-Formation Assay

The cells (1×10^4 cells) were cultured in a 100-mm petri dish and incubated for 10 days with 10 mL medium, and adding 1 mL medium every other day. The colonies were then fixed with methanol for 10 min, then stained with 0.5% crystal violet for 10 min. The cells were then washed twice with phosphate buffered saline (PBS) at room temperature. Photomicrographs were then taken after dish dried.

2.5 Migration Assay

SKOV3-Vector/ID8-Vector cells and SKOV3-SPARC/ID8-SPARC cells (SKOV3: 8×10^5 cells per well; ID8: 3×10^5 cells per well) were added to the upper chamber in one 24-well Transwell plate (Corning, Corning, NY, USA) with serum-free medium. Fetal bovine serum (FBS) (10%) was added to the lower chamber. After 24 h, the cells that migrated into the lower chamber were fixed with methanol and stained with 0.5% crystal violet. Photomicrographs were taken through a light microscope (EVOS, ThermoFisher, Waltham, MA, USA), and ImageJ software was used to count cells.

2.6 Cell Counting Kit-8 (CCK-8) Assay

SKOV3-Vector/ID8-Vector cells and SKOV3-SPARC/ID8-SPARC cells were seeded into 96-well plates at 5×10^3 cells. CCK-8 (10%) (Beyotime, Shanghai, China) as added to each well on Days 1, 2, and 3. The cells were incubated for 30 min at 37 °C and read at 450 nm by a plate reader.

2.7 Cell-Adhesion Assay

A 24-well plate was precoated with 100 μ L fibronectin (20 μ g/mL), 100 μ L collagen I (100 μ g/mL), and 100 μ L poly-l-lysine (100 μ g/mL) in PBS, and placed in a cell incubator for 1 h. The PBS was replaced and 300 μ L blocking buffer (0.5% bovine serum albumin (BSA) in medium) was added to each well for an additional 60 min. Then, the blocking buffer was replaced with 1×10^5 cells per well (SKOV3-Vector/ID8-Vector cells and SKOV3-SPARC/ID8-SPARC cells) in serum-free medium. After incubating in the cell incubator for 30 min, the medium was wiped out, and the adherent cells were fixed for 5 min with 100 μ L methanol. The cells were then stained with 100 μ L of 0.5% crystal violet for 5 min. Finally, the plate was flushed with PBS and air-dried. Photomicrographs were taken and the cells were counted by ImageJ software.

2.8 Soft Agar Spheroid-Formation Assay

Agarose solution (1%) was prepared and autoclaved, then spread on the bottom of the 100-mm dish when the temperature dropped to about 40 °C. The cells (1×10^4 cells) were seeded and incubated in a 100-mm dish with complete medium for 5 days until the cells formed spheres. Then, these cells were poured into another 100-mm dish without agarose coating, and incubated in the same condition for 10 days.

2.9 Pan-Cancer Data Mining of SPARC

UCSC Xena and Genotype-Tissue Expression (GTEx) databases were explored by UCSCXenaShiny, an R software package (version 4.23, Lucent Technologies, Murray Hill, NJ, USA) [16]. The mRNA expression and DNA methylation of SPARC were screened with this application (Plugin Version: v0.1.0) in both tumor samples and nor-

mal samples, if any. A $p \leq 0.05$ was considered statistically significant. The correlation between SPARC mRNA with immune signatures was analyzed with a Spearman test using signatures of Tumor Immune Estimation Resource (TIMER) database, including T cell CD4⁺, T cell CD8⁺, myeloid dendritic cell, neutrophil, macrophage, and B cell, were calculated. A related heatmap was plotted with p values. Similarly, SPARC mRNA level correlations with Stemness, tumor mutation burden (TMB), and microsatellite instability (MSI) were calculated. A circle map of correlation values was plotted. Moreover, the mRNA expression level of SPARC in TCGA and GTEx databases was extracted and highlighted in a violin plot for ovarian cancer.

2.10 Gene Expression Profiling Interactive Analysis (GEPIA)

GEPIA is a customizable pan-cancer analysis online tool for sequencing data from TCGA with clinical parameters. The GEPIA database was accessed to obtain SPARC transcript expressions among the major stages of ovarian cancer sorted by transcripts per million [17]. An F value was calculated.

2.11 Survival Analysis Validation of SPARC

The Kaplan-Meier plotter for ovarian cancer was accessed to evaluate SPARC expression value with clinical outcome [18]. The probe SPARC (212667_at) was used for estimating overall survival or progression-free survival by the Kaplan-Meier method. A positive independent biomarker was considered as log-rank $p \leq 0.05$ as a threshold. In addition, specific drug-based overall survivals (Platin, taxane, docetaxel, paclitaxel, gemcitabine) were also calculated.

2.12 Drug Response Analysis of SPARC

Frequent genetic mutations in ovarian-cancer are considered one of the main reasons for extremely poor clinical outcome. The ROC plotter database (website database with therapy effect associated with sequencing data of cancers) was accessed to explore the general drug response for chemical application in treating ovarian cancer. SPARC (200665_s_at) was validated in both drug-responder and non-responder cohorts, and the Area Under Curve (AUC) with p -value was calculated [19]. In addition, specific drugs (Platin, taxane, docetaxel, paclitaxel, gemcitabine) were applied by ROC plotter in both drug-response and non-response cohort. The relapse-free survival value at 6 mo ($n = 1347$) was set as the analysis cohort.

2.13 SPARC Correlation with Immune Cell Infiltration Analysis

The Timer2.0 database was accessed to provide an estimation of immune infiltration with SPARC level. The Immune association model was applied for evaluation of the

correlation of SPARC expression (log2 TPM (transcripts per kilobase million)) with infiltration of 9 major immune cell types (B cell; T cell CD4⁺; T cell CD8⁺; macrophage; cancer-associated fibroblast; natural killer (NK) cell; mast cell; myeloid dendritic cell; neutrophil) in ovarian cancer. The Rho with p value was calculated.

2.14 Correlation between EMT Signature Genes and SPARC

The Timer2.0 database was applied using cancer exploration model [20]. The correlation between SPARC RNA-seq expression (log2 TPM) and CD274, CDH1, CDH2, CTNNB1, FN1, MMP2, MMP9, VIM, ZEB1, and MUC1 were calculated by Pearson correlation with a p value. The immune checkpoint genes *CTLA4* and *PDCD1* were also counted with SPARC expression.

2.15 Identification of DEGs (Differentially Expressed Genes) and GO/KEGG (Gene Ontology/Kyoto Encyclopedia of Genes and Genomes) Enrichment

The LinkedOmics online database was used for the identification of DEGs. The methods were previously described [21]. Briefly, the Pearson correlation of SPARC with all RNA-seq transcripts was calculated. All positive-Pearson value related DEGs ($p \leq 0.01$) were selected for GO and KEGG enrichment analysis.

2.16 Prediction of Potential Targeted Drugs Based on SPARC Expression

The Drug-Gene Interaction Database (<https://www.dgidb.org/>) is an online webtool that contains genetic information on drug-gene interactions, based on the biomarkers of target therapy for ovarian cancer [22]. Using the high or low expression of SPARC with the median value of the database cohort, the drug response for ovarian cancer patients was calculated.

2.17 Statistical Analysis

Two groups were compared with Prism software (GraphPad, San Diego, CA, USA) using a two-tailed unpaired Student's t -test. All data were represented as mean \pm standard error of the mean (SEM). Differences were considered statistically significant if $p \leq 0.05$.

3. Results

3.1 SPARC is Differentially Expressed and Related to Immune Signatures in a Pan-Cancer Analysis

According to the pan-cancer expression analysis comparing tumor and normal tissue, SPARC is differentially expressed in ACC, BRCA, CESC, CHOL, COAD, DLBC, ESCA, GBM, HNSCC, KIRC, KIRP, LAML, LGG, LIHC, OV, PAAD, PRAD, READ, SKCM, STAD, THCA, THYM, and UCEC. With the exception of CESC, PRAD, and UCEC, the cancer subtypes showed an increased expression of SPARC (Fig. 1A). It is interesting

that the DNA methylation of SPARC did not affect mRNA higher expression in tumor. The beta-value was higher in BLCA, BRCA, CESC, CHOL, ESCA, HNSCC, KIRC, KIRP, LUAD, LUSC, PAAD, PCPG, PRAD, and UCEC (Fig. 1B). This inconsistent status between mRNA expression and DNA methylation indicated post-transcriptional modification of SPARC. Importantly, SPARC is generally positively correlated with immune signatures (TIMER). In ovarian cancer, SPARC expression is positively related to T cell CD8⁺, T cell CD4⁺, neutrophil, myeloid dendritic cell, and macrophage, and negatively related with B cell (Fig. 1C). SPARC shows no association with TMB and MSI status (Fig. 1E,F). However, SPARC is generally negative with tumor stemness indicating potential differential functions (Fig. 1D).

3.2 SPARC is a Prognostic Marker in Ovarian Cancer and Related to Conventional Chemical Drug Response

SPARC was significantly increased in ovarian cancer tumor samples comparing normal ovarian tissue from the TCGA/GTEX database (Fig. 2A). According to the major-stage analysis, SPARC increased from early stages to late stages, $F = 1.19$ (Fig. 2B). Although the dataset lacks Stage I data, the other major stages from Stage IIa to Stage IV have already shown the increased expression pattern with advancing stages. The Kaplan–Meier (KM)-plot results showed that SPARC expression could be used as an ovarian cancer prognostic marker for both overall survival and progression-free survival predictions, $p = 0.006$ and 0.0013 , respectively (Fig. 2C,D). It is important that the higher expression group demonstrated a worse clinical outcome in overall survival and progression-free survival prediction [hazard ratio (HR) = 1.19 and 1.24, respectively]. For general chemical drug response based on SPARC expression level, the bar plot shows that the non-response group had a higher expression than did the response group (Fig. 2E). Receiver operating characteristic (ROC) analysis showed an AUC = 0.585, with $p = 5 \times 10^{-4}$ (Fig. 2F).

For specific drug-response-based survival analysis, including Platin, taxane, cocetaxel, paclitaxel, and gemcitabine, SPARC gene expression showed a consistent increase in the non-responder group and a worse clinical outcome. Platin-treated patients (Fig. 3A): AUC = 0.594 with $p = 1.7 \times 10^{-4}$, and overall survival with a logrank $p = 2.2 \times 10^{-6}$. Taxane-treated patients (Fig. 3B): AUC = 0.594 with $p = 1.2 \times 10^{-3}$, and overall survival with a logrank $p = 8.3 \times 10^{-7}$. Docetaxel-treated patients (Fig. 3C): AUC = 0.726 with $p = 0.1$, and overall survival with a logrank $p = 7.3 \times 10^{-2}$. Paclitaxel-treated patients (Fig. 3D): AUC = 0.53 with $p = 0.31$, and overall survival with a logrank $p = 3.4 \times 10^{-2}$. Gemcitabine-treated patients (Fig. 3E): AUC = 0.531 with $p = 0.39$, and overall survival with a logrank $p = 6.9 \times 10^{-1}$.

3.3 SPARC Regulates Ovarian Cancer Cell Proliferation, Migration, and Adhesion

For SKOV3 cells, the CCK-8 test demonstrated that overexpression of SPARC at Day 3 significantly increased cell proliferation (Fig. 4A). For the ID8 cell line, overexpressed SPARC produced a significantly increased proliferation at Days 2 and 3 (Fig. 4B). The cell migration ability was evaluated by Transwell, and the wound-healing assay showed that SPARC overexpression promoted cell movement in both SKOV-3 and ID8 ovarian cancer cells (Fig. 4C,E,F). For cell-colony formation and ovarian-cancer-spheroid formation, increased SPARC level enhanced the cell colony and spheroid-formation numbers in both SKOV-3 and ID8 cells (Fig. 5A,B). For cell-to-matrix adhesion, increased SPARC raised extracellular matrix collagen I, fibronectin, and Poly-L-lysine in ovarian cancer cell lines SKOV-3 and ID8 (Fig. 5D,E). Those *in vitro* experiments validated the GO biological process enrichment result including terms as “cell adhesion, positive regulate cell migration, positive regulation of ERK1 and ERK2 cascade, cell migration, and cell-matrix adhesion” (Fig. 4D). For KEGG enrichment, the terms “focal adhesion, ECM-receptor interaction, cell adhesion molecules, MAPK signaling pathway, and regulation of actin cytoskeleton” were indicated by those cell phenotypes (Fig. 5C).

3.4 SPARC Expression Level is Associated with Immune Cell Infiltration and EMT Signatures

SPARC level was significantly negatively related to B cell infiltration, with a $Rho = -0.306$ and $p = 8.8 \times 10^{-7}$. Similarly, SPARC expression was also negatively associated with infiltration of mast cells and CD4⁺ T cells, with $Rho = -0.128$ and $Rho = -0.128$, and $p = 4.44 \times 10^{-2}$ and $p = 4.30 \times 10^{-2}$, respectively. In contrast, higher SPARC level was positively related to CD8⁺ T cell, macrophage, cancer associated fibroblast, NK cell, myeloid dendritic cell, and neutrophil infiltration levels (Fig. 6). For EMT signatures, SPARC level was strongly associated with CD274, CTNNB1, FN1, MMP2, MMP9, VIM, and ZEB1, indicating a metastasis possibility. However, there were no significant effects for CDH1, CDH2, and MUC1 (Fig. 7). In addition, SPARC was related to immune checkpoint gene *CTLA4* ($Rho = 0.25$; $p = 1.09 \times 10^{-5}$) and *PDCDI* ($Rho = 0.191$; $p = 8.44 \times 10^{-4}$).

3.5 SPARC Level is not Related to Current Target Therapeutic Drugs Based on Specific Mutation Genes

Aside from the ABL- (Abelson Murine Leukemia Viral Oncogene Homolog) targeted drug AZD0530 (Fig. 8), all other drug effect predictions showed negative results, including paclitaxel ($n = 26$). This may have been due to the small number of patients.

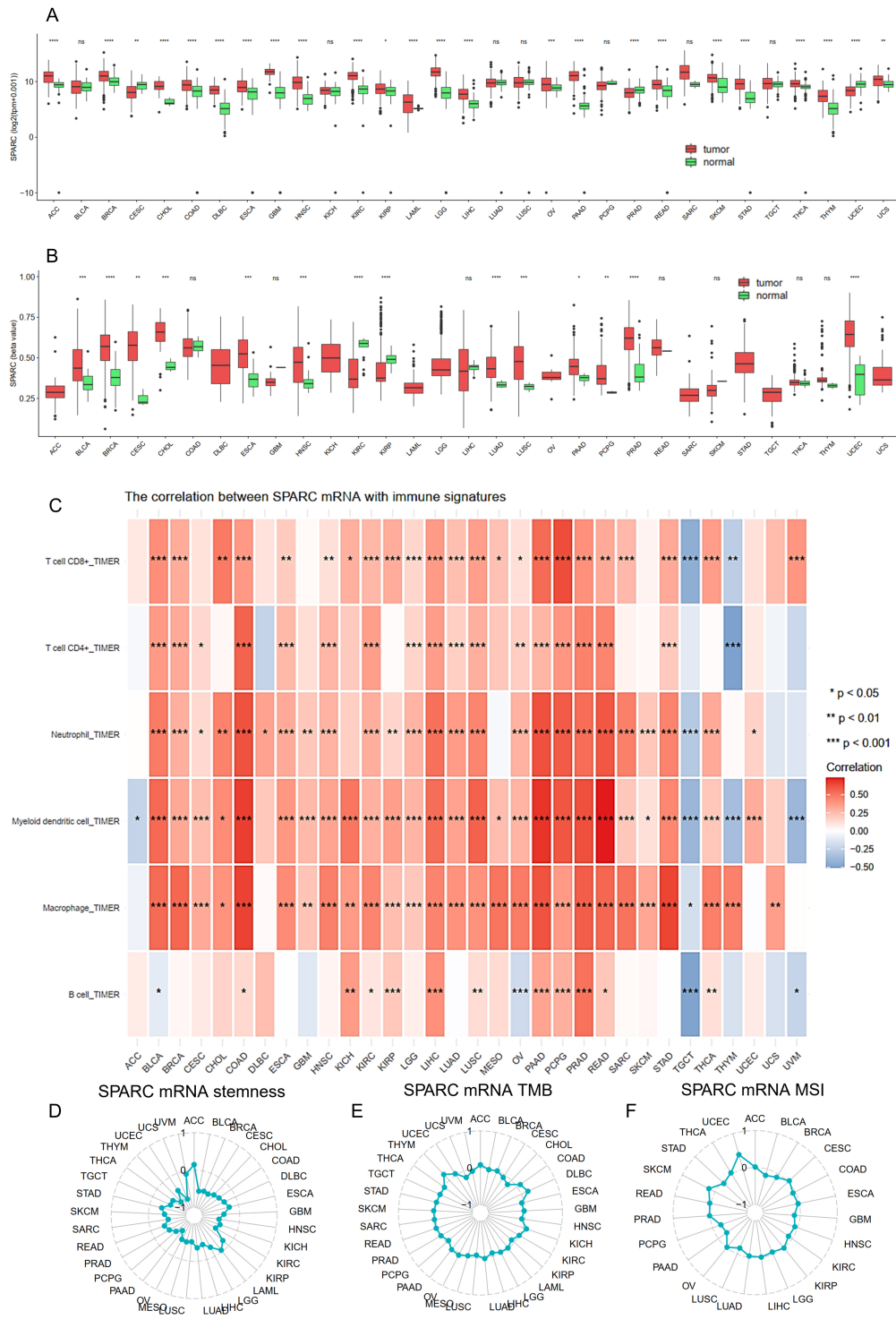


Fig. 1. Pan-cancer analysis of SPARC. (A) Bar plot of SPARC (secreted protein, acidic and rich in cysteine) expression in tumors from The Cancer Genome Atlas (TCGA) in tumor sample and normal tissue. TPM, Transcripts Per Kilobase Million. (B) The DNA methylation of SPARC (TCGA database) for tumor and normal tissue using a bar plot with beta value. (C) The heatmap of the correlation between SPARC mRNA with immune signature in Pan-cancer. (D) The circle map of the correlation between SPARC mRNA level and cancer stemness through a Pan-cancer analysis. (E) The correlation circle map of SPARC mRNA level and tumor mutational burden (TMB) in Pan-cancer. (F) The correlation circle map of SPARC mRNA level and microsatellite instability (MSI) through Pan-cancer analysis. Inner circle indicates correlation = -1, middle circle indicates correlation = 0, outer circle indicates correlation = 1. Cancer type TCGA study abbreviation list: <https://gdc.cancer.gov/resources-tcga-users/tcga-code-tables/tcga-study-abbreviations>.

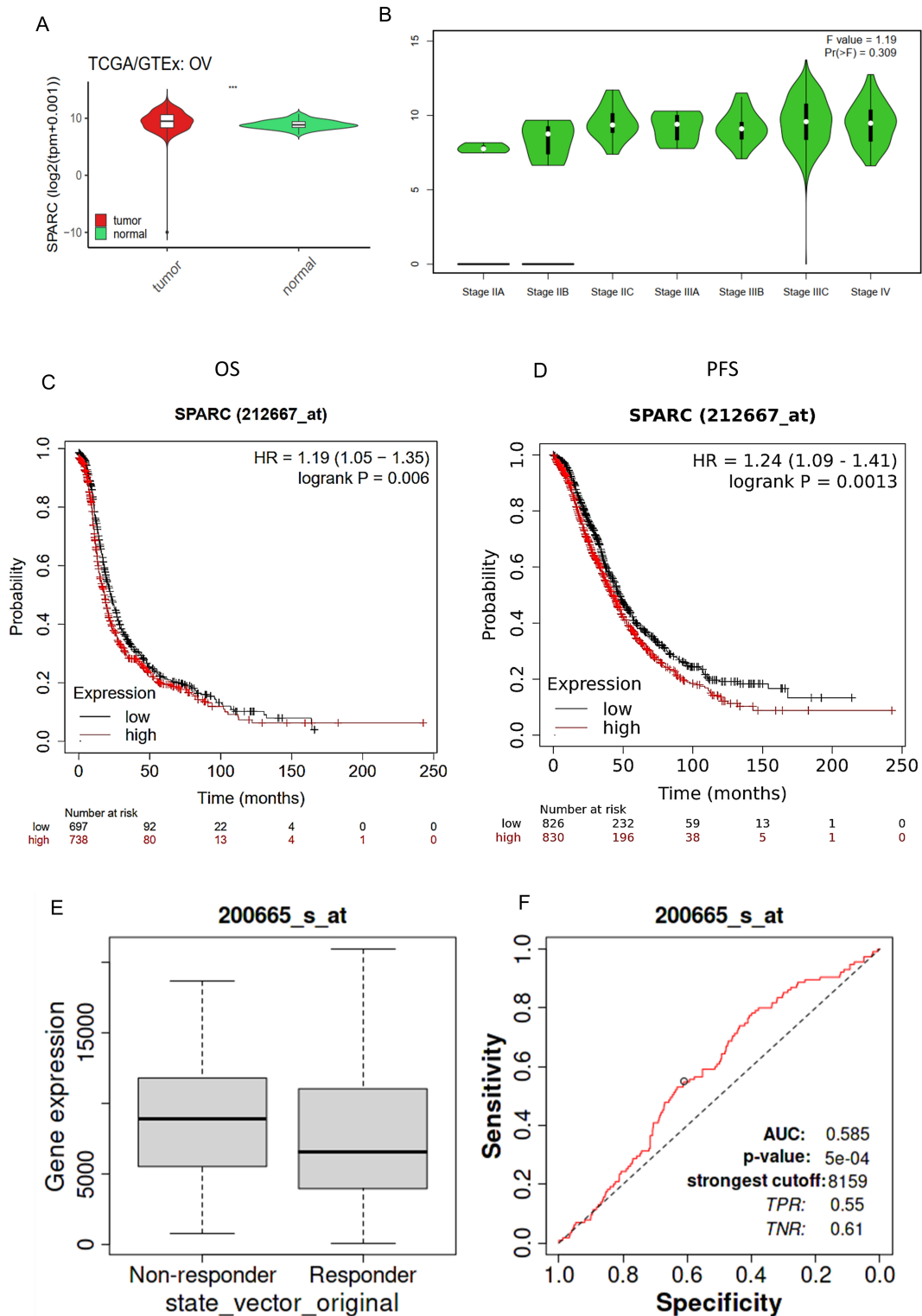


Fig. 2. SPARC as a biomarker of ovarian cancer. (A) Bar plot of SPARC expression comparing ovarian carcinoma (OV) tumor and normal tissue. (B) A violin plot of SPARC expression in ovarian carcinoma major stages. Pr (> F), the association between the significance probability value and the F Value. (C) The Kaplan–Meier (KM)-plot result of OS using SPARC (212667_at) in ovarian cancer. (D) The KM-plot result of progression-free survival (PFS) using SPARC (212667_at) in ovarian cancer. (E) Box plot of SPARC gene expression level in both non-responder and responder group of chemical treatments. (F) The receiver operating characteristic (ROC) plot of SPARC in predicting general chemical drug response. TCGA/GTEX, The Cancer Genome Atlas/Genotype-Tissue Expression; OS, overall survival; PFS, progressions-free survival; HR, hazard ratio; AUC, Area Under Curve; TPR, true positive rate; TNR, true negative rate.

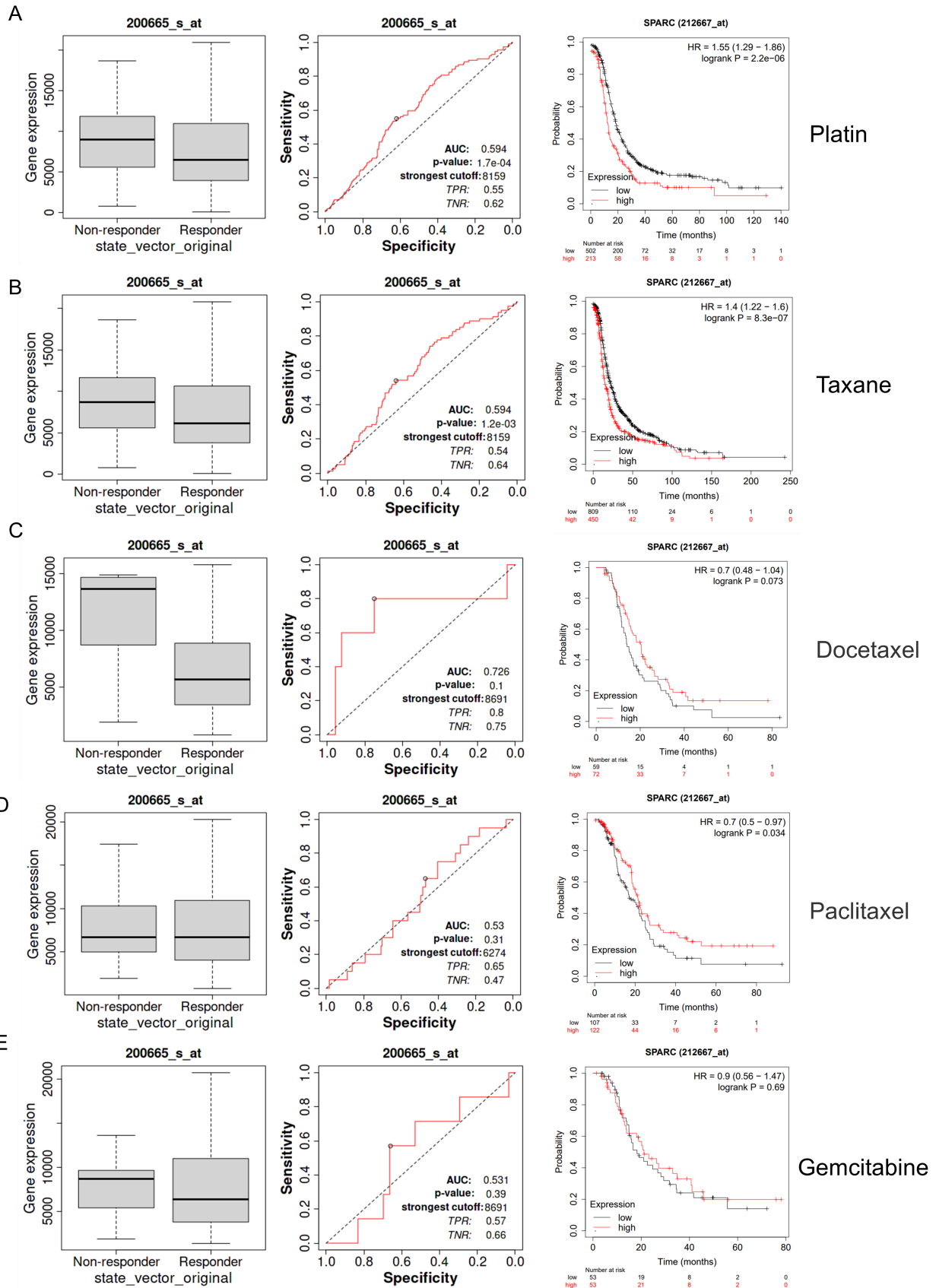


Fig. 3. SPARC as drug response indicator of ovarian cancer. (A) A box plot of *SPARC* gene expression in both the non-responder and responder group of Platin treatment. ROC plot and drug based overall survival KM-plot (Best *p*-value). (B) Taxane. (C) Docetaxel. (D) Paclitaxel. (E) Gemcitabine.

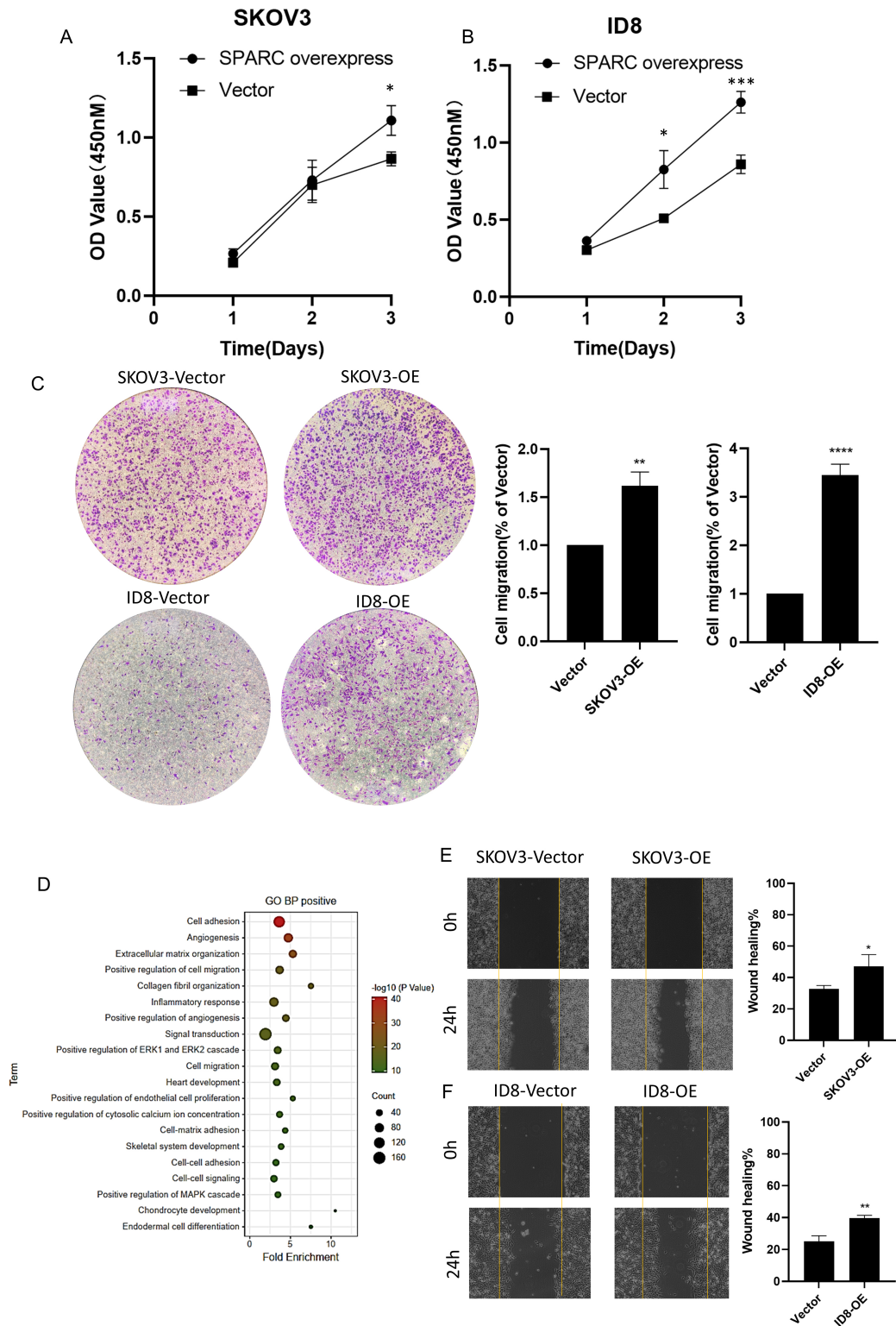


Fig. 4. SPARC promoting ovarian cancer cell proliferation and migration. (A) Cell Counting Kit-8 (CCK-8) dot plot of cell proliferation in SKOV3 cells. *indicates $p < 0.05$. (B) CCK-8 dot plot of cell proliferation in ID8 cells. ***indicates $p < 0.001$. (C) Transwell assay showing increasing SPARC (over-expression (OE) group) enhanced cell migrations rate under starving status in both SKOV-3 and ID8 cells. (D) Bubble plot of Gene Ontology (GO) biological process analysis. (E,F) The wound healing assay showed results consistency with Transwell assay results in evaluation of SKOV-3 and ID8 cell migration by increasing SPARC expression level at 24 h. Yellow line indicates starting point. *indicates $p < 0.05$, **indicates $p < 0.01$, ***indicates $p < 0.001$, ****indicates $p < 0.0001$.

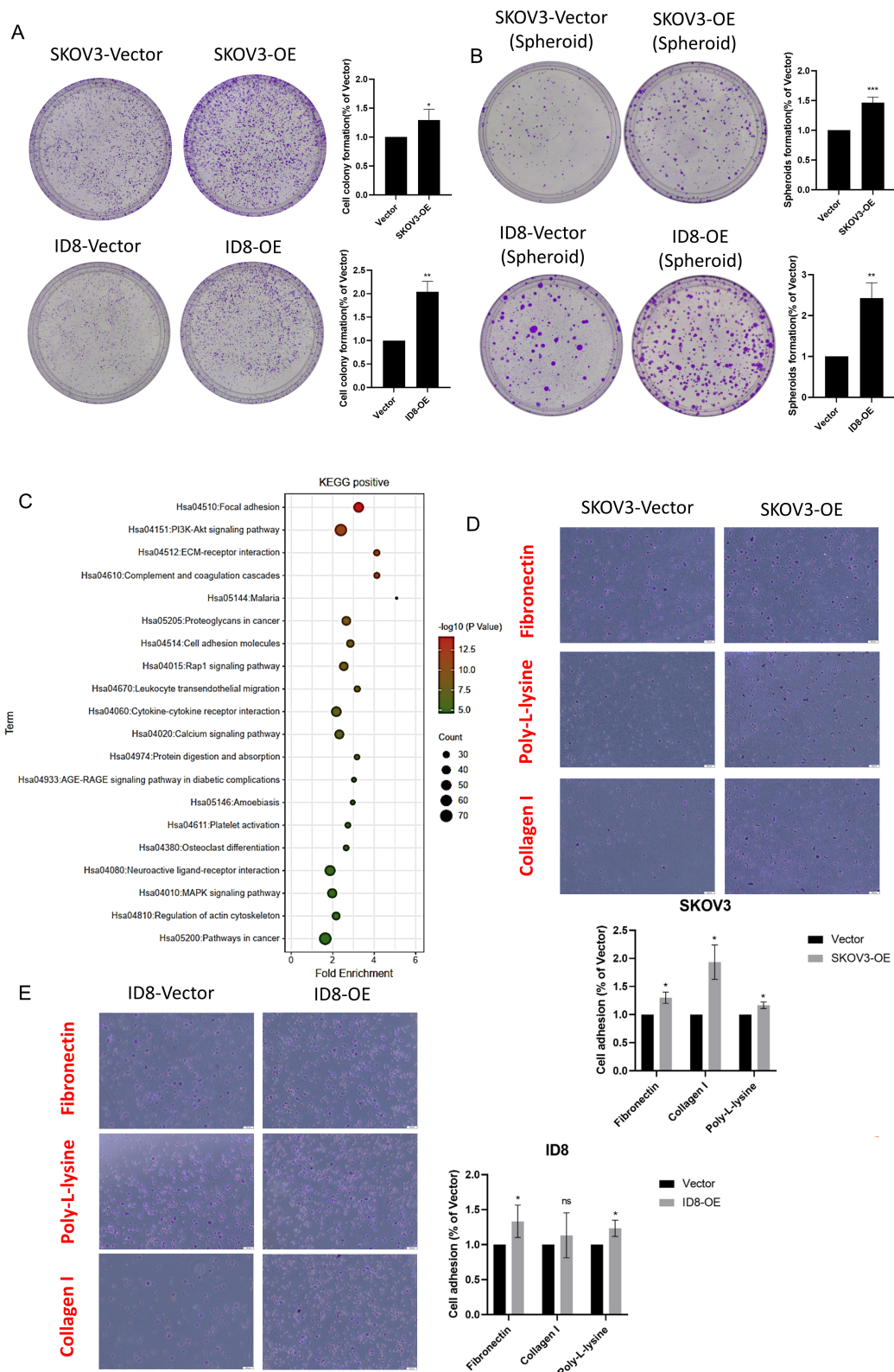


Fig. 5. SPARC regulating ovarian cancer spheroids formation and adhesion to matrix. (A) Colony-formation assay results: SPARC increase promoted colony numbers in SKOV-3 and ID8 cells. (B) Spheroid-formation assay supported SPARC level was associated with cell survival during metastasis process forming mediated spheroids. (C) Bubble plot of Kyoto Encyclopedia of Genes and Genomes (KEGG) enrichment demonstrated major that a signaling pathway was involved. (D,E) Cell-to-matrix adhesion test showed that higher SPARC level regulated SKOV-3 and ID8 cells adherence capability to extracellular matrix. *indicates $p < 0.05$, **indicates $p < 0.01$, ***indicates $p < 0.001$, ns = not significant.

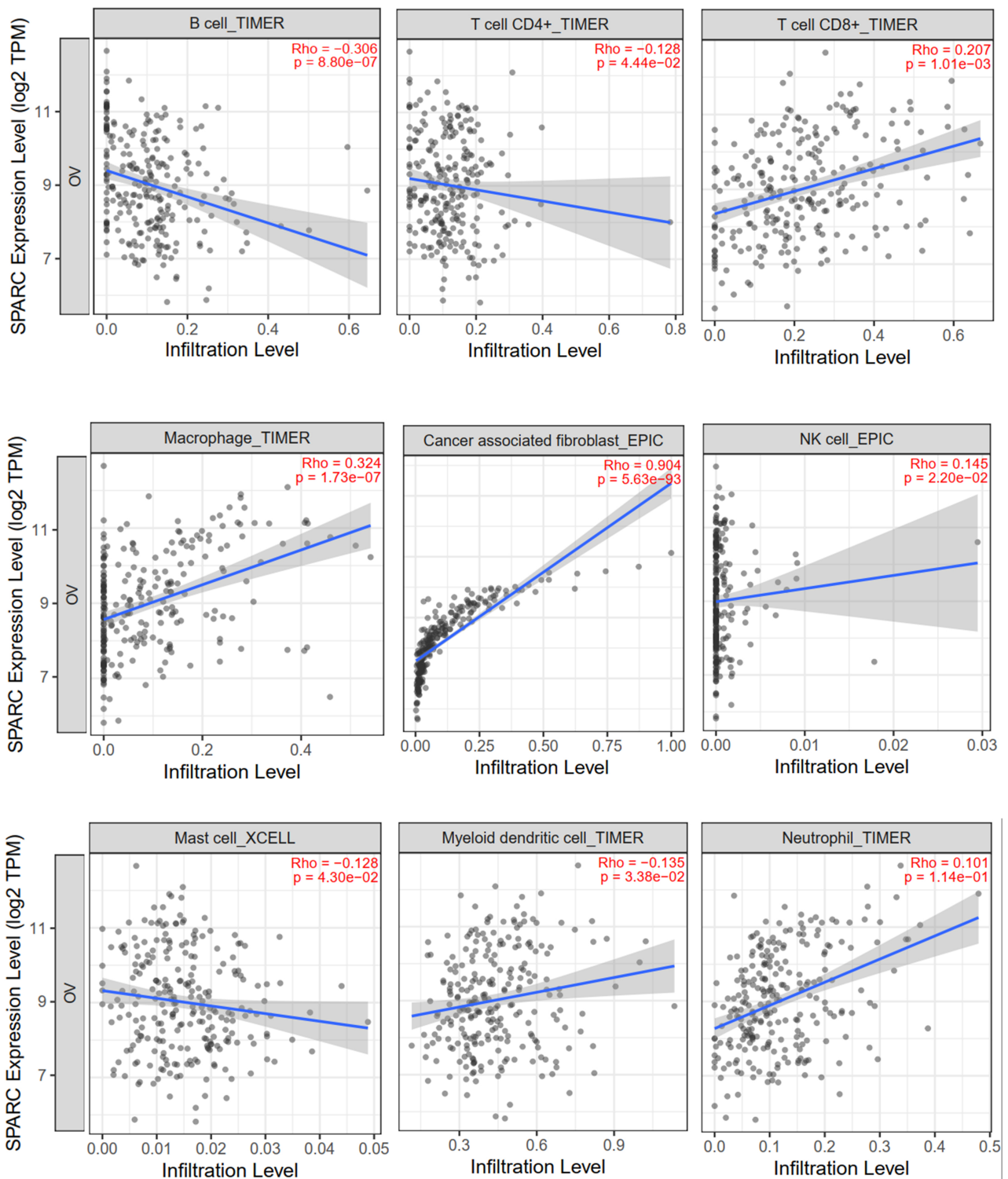


Fig. 6. SPARC expression related correlation with specific immune cell type infiltration. Rho = Spearman's correlation.

4. Discussion

Although cancer therapy has improved, ovarian cancer is still the leading cause of female carcinoma-associated death. So far, the major problem is the lack of effective molecular targets and biomarkers. SPARC is differentially expressed in cancers and adjacent tissues. It has been re-

ported that SPARC expression was significantly elevated in liver, prostate, breast, and colorectal cancers. However, the reported role of SPARC is quite unclear based on contextualization [10]. Evidence has shown that increased SPARC could promote cancer cell proliferation and metastasis, and result in worse clinical outcomes for solid neoplasms including ovarian cancer [8,13,23].

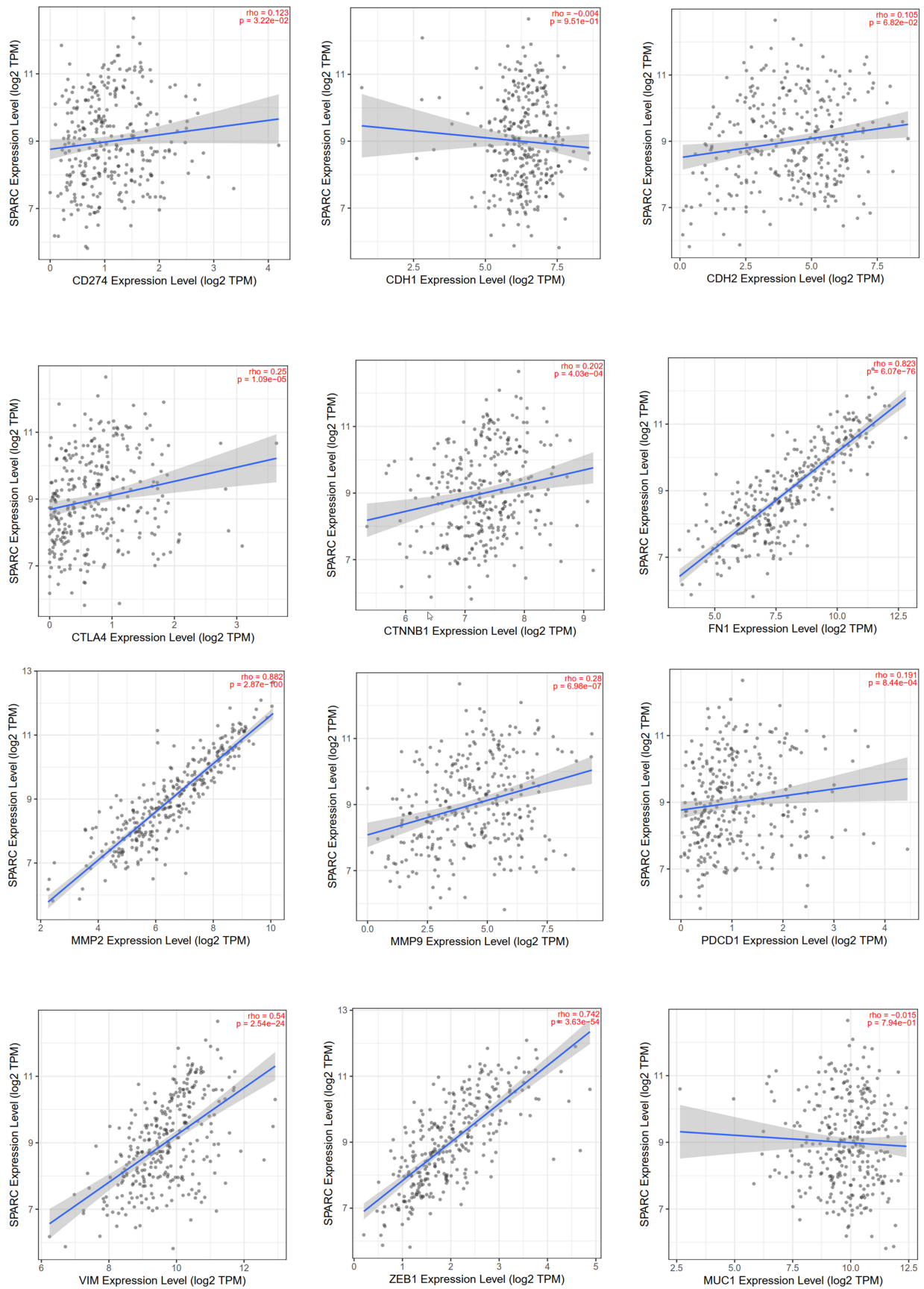


Fig. 7. The correlation dot plot between SPARC level and epithelial-mesenchymal transition (EMT)/immune checkpoint signature markers. Rho = Spearman's correlation.

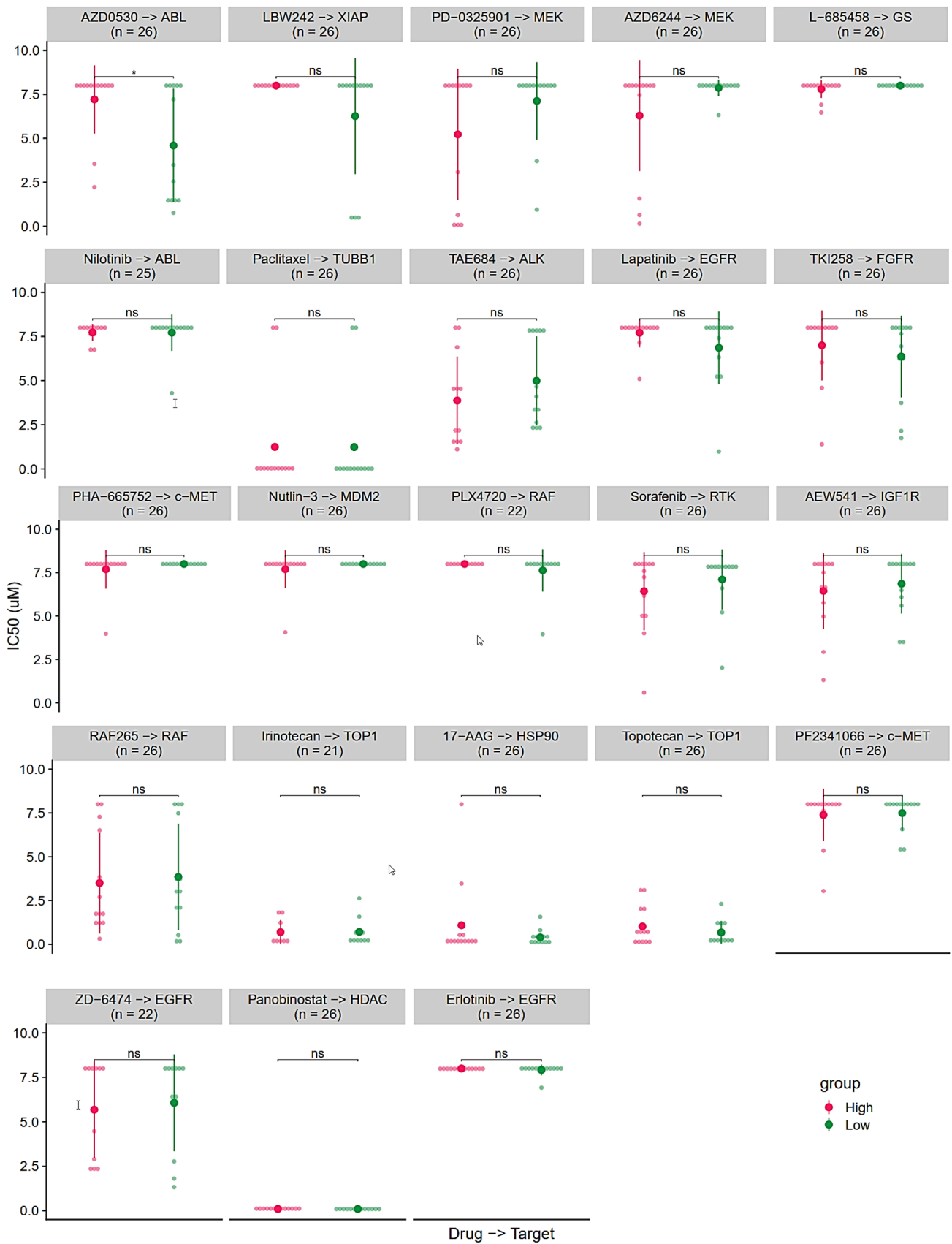


Fig. 8. Target drugs response prediction result using SPARC expression level. Red group: Higher expression than median. Green group: Lower expression than median. *indicated $p < 0.05$, ns = not significant.

Our *in vitro* study findings supported the notion that SPARC acts as an oncogene that functions primarily by increasing the adhesive ability of forming spheroids as well as increasing proliferation in ovarian cancer. SPARC significantly enhances ovarian cancer adhesion to the ECM molecules. It is noteworthy that SPARC promoter hypermethylated usually resulted a decreased of mRNA expression, but compared with normal tissue the mRNA expression of SPARC in tumor was detected increasing, which requires further investigation. There is evidence that expression of SPARC was related to cancer malignancy behaviors. It should be noted that the stromal cells that expressed high levels of SPARC also have inactivation of the SPARC promoter, in turn leading to a worse clinical outcome. Also, SPARC level is related to tumor microenvironment, including immune responses, but the results are quite controversial.

We performed comprehensive bioinformatic analysis based on sequencing data, as well as ROC analysis for drug-based survival prediction, to reveal the integrated role of SPARC in ovarian cancer for prognostic value, drug treatment response, and immune characterized modulating function. Our findings suggest that high SPARC expression level indicates poor clinical outcomes and higher malignancy. We found that SPARC expression level could be used independently as a prognostic marker for overall survival and progression-free survival predictions, which supported previous reports [18]. Additionally, higher expression of SPARC generally could be considered as a poor drug-response indicator for chemical therapy. However, no specific target drugs could be useful for using SPARC as an evaluation drug other than saracatinib (AZD0530).

Our present study has some limitations. In view of the insufficient pathological data, we did not analyze the immunohistochemistry of SPARC expression in the paraffin-embedded samples of ovarian cancer patients. We also did not validate the carcinogenic effects of SPARC in an animal model due to limited time and funds. In future work, we intend to further verify the involvement of SPARC in the PI3K-AKT and MAPK signaling pathways in ovarian cancer cells *in vitro*, run supplement animal experiments, and further validate pathological specimens.

In general, SPARC, in both our results and in previous reports, should be noted as a novel oncogene prompting cancer cell EMT, and frequently causing metastasis and poor clinical outcomes [9,13,15]. In relation to the tumor microenvironment, SPARC enhanced cancer adhesive capability by improving spheroid formation and attachment to the extracellular matrix. Those phenotypes may be supported by PI3K-AKT and MAPK signaling pathways. In addition, the role of SPARC in interaction with immune cell infiltration is still not clear. Therefore, the biological role of SPARC in ovarian cancer merits further in-depth investigation.

5. Conclusions

SPARC promotes ovarian cancer progression via proliferation, migration, invasiveness, clonality, and stemness, which are related to PI3K-AKT and MAPK signaling pathways. High expression of SPARC in ovarian cancer patients can be used as a marker of poor prognosis and poor drug response. High SPARC expression is positively correlated with immune signatures; the mechanism for this is not clear and requires further investigation.

Availability of Data and Materials

The datasets used and/or analyzed during the current study are available from the corresponding author on reasonable request.

Author Contributions

XG performed literature search, drafted the manuscript and figures; and HT performed the bioinformatic analysis, drafted the manuscript and figures. XL performed the *in vitro* experiments and drafted the manuscript. PL and JL helped in analysis and interpretation of data and revised the manuscript. SY designed concept of the study and revised the whole manuscript. All authors have read and agreed to the published version of the manuscript.

Ethics Approval and Consent to Participate

Not applicable.

Acknowledgment

We thank all who help us in writing the manuscript.

Funding

This study was supported by Research Project of China Primary Health Care Foundation.

Conflict of Interest

The authors declare no conflict of interest.

References

- [1] Vaz J, Ansari D, Sasor A, Andersson R. SPARC: A Potential Prognostic and Therapeutic Target in Pancreatic Cancer. *Pancreas*. 2015; 44: 1024–1035.
- [2] Said N. Roles of SPARC in urothelial carcinogenesis, progression and metastasis. *Oncotarget*. 2016; 7: 67574–67585.
- [3] Wu L, de Perrot M. Omics Overview of the SPARC Gene in Mesothelioma. *Biomolecules*. 2023; 13: 1103.
- [4] Li XL, Li JL, Qiu DJ, Ma L. Methylation-mediated expression of SPARC is correlated with tumor progression and poor prognosis of breast cancer. *Neoplasma*. 2022; 69: 794–806.
- [5] Li L, Zhu Z, Zhao Y, Zhang Q, Wu X, Miao B, *et al.* FN1, SPARC, and SERPINE1 are highly expressed and significantly related to a poor prognosis of gastric adenocarcinoma revealed by microarray and bioinformatics. *Scientific Reports*. 2019; 9: 7827.

- [6] Sun W, Feng J, Yi Q, Xu X, Chen Y, Tang L. SPARC acts as a mediator of TGF- β 1 in promoting epithelial-to-mesenchymal transition in A549 and H1299 lung cancer cells. *BioFactors* (Oxford, England). 2018; 44: 453–464.
- [7] Pang MF, Georgoudaki AM, Lambut L, Johansson J, Tabor V, Hagikura K, *et al.* TGF- β 1-induced EMT promotes targeted migration of breast cancer cells through the lymphatic system by the activation of CCR7/CCL21-mediated chemotaxis. *Oncogene*. 2016; 35: 748–760.
- [8] Bao JM, Dang Q, Lin CJ, Lo UG, Feldkoren B, Dang A, *et al.* SPARC is a key mediator of TGF- β -induced renal cancer metastasis. *Journal of Cellular Physiology*. 2021; 236: 1926–1938.
- [9] Chang CH, Yen MC, Liao SH, Hsu YL, Lai CS, Chang KP, *et al.* Secreted Protein Acidic and Rich in Cysteine (SPARC) Enhances Cell Proliferation, Migration, and Epithelial Mesenchymal Transition, and SPARC Expression is Associated with Tumor Grade in Head and Neck Cancer. *International Journal of Molecular Sciences*. 2017; 18: 1556.
- [10] Camacho D, Jesus JP, Palma AM, Martins SA, Afonso A, Peixoto ML, *et al.* SPARC-p53: The double agents of cancer. *Advances in Cancer Research*. 2020; 148: 171–199.
- [11] Sailaja GS, Bhoopathi P, Gorantla B, Chetty C, Gogineni VR, Velpula KK, *et al.* The secreted protein acidic and rich in cysteine (SPARC) induces endoplasmic reticulum stress leading to autophagy-mediated apoptosis in neuroblastoma. *International Journal of Oncology*. 2013; 42: 188–196.
- [12] Said N, Frierson HF, Sanchez-Carbayo M, Brekken RA, Theodorescu D. Loss of SPARC in bladder cancer enhances carcinogenesis and progression. *The Journal of Clinical Investigation*. 2013; 123: 751–766.
- [13] Chen J, Wang M, Xi B, Xue J, He D, Zhang J, *et al.* SPARC is a key regulator of proliferation, apoptosis and invasion in human ovarian cancer. *PloS One*. 2012; 7: e42413.
- [14] John B, Naczki C, Patel C, Ghoneum A, Qasem S, Salih Z, *et al.* Regulation of the bi-directional cross-talk between ovarian cancer cells and adipocytes by SPARC. *Oncogene*. 2019; 38: 4366–4383.
- [15] Said N, Socha MJ, Olearczyk JJ, Elmarakby AA, Imig JD, Mottamed K. Normalization of the ovarian cancer microenvironment by SPARC. *Molecular Cancer Research: MCR*. 2007; 5: 1015–1030.
- [16] Wang S, Xiong Y, Zhao L, Gu K, Li Y, Zhao F, *et al.* UCSCXenaShiny: an R/CRAN package for interactive analysis of UCSC Xena data. *Bioinformatics* (Oxford, England). 2022; 38: 527–529.
- [17] Tang Z, Li C, Kang B, Gao G, Li C, Zhang Z. GEPIA: a web server for cancer and normal gene expression profiling and interactive analyses. *Nucleic Acids Research*. 2017; 45: W98–W102.
- [18] Györfy B. Discovery and ranking of the most robust prognostic biomarkers in serous ovarian cancer. *GeroScience*. 2023; 45: 1889–1898.
- [19] Fekete JT, Györfy B. ROCplot.org: Validating predictive biomarkers of chemotherapy/hormonal therapy/anti-HER2 therapy using transcriptomic data of 3,104 breast cancer patients. *International Journal of Cancer*. 2019; 145: 3140–3151.
- [20] Li T, Fu J, Zeng Z, Cohen D, Li J, Chen Q, *et al.* TIMER2.0 for analysis of tumor-infiltrating immune cells. *Nucleic Acids Research*. 2020; 48: W509–W514.
- [21] Vasaikar SV, Straub P, Wang J, Zhang B. LinkedOmics: analyzing multi-omics data within and across 32 cancer types. *Nucleic Acids Research*. 2018; 46: D956–D963.
- [22] Cotto KC, Wagner AH, Feng YY, Kiwala S, Coffman AC, Spies G, *et al.* DGIdb 3.0: a redesign and expansion of the drug-gene interaction database. *Nucleic Acids Research*. 2018; 46: D1068–D1073.
- [23] Gao ZW, Liu C, Yang L, He T, Wu XN, Zhang HZ, *et al.* SPARC Overexpression Promotes Liver Cancer Cell Proliferation and Tumor Growth. *Frontiers in Molecular Biosciences*. 2021; 8: 775743.